



Thermo-Responsive and Shape-Adaptive Hydrogel Actuators from Fundamentals to Applications

Yanxian Zhang,^{1,5*} Shaowen Xie,^{1,5*} Dong Zhang,^{5†} Baiping Ren,⁵ Yonglan Liu,⁵ Li Tang,¹ Qiang Chen,² Jintao Yang,³ Jiang Wu,^{4*} Jianxin Tang^{1*} and Jie Zheng^{5*}

Shape adaptable hydrogel actuators, capable for changing their shapes in response to single or multiple thermo/other external stimulus, are considered as new emerging smart materials for a broad range of fundamental/industrial research and applications. This review mainly focuses on the recent progress (particularly over the past 5 years) on such thermo-responsive hydrogel actuators. Recent fundamental advances and engineering applications in materials design/synthesis/characterization, distinct actuation mechanisms, and intriguing examples of these hydrogel actuators of single or dual stimuli are selectively presented. Specific or general design principles for thermo-induced hydrogel actuators are also provided to better illustrate the structure-property relationship. In the end, we offer some personal perspectives on current major challenges and future research directions in this promising field. Overall, this review discusses current status, progress, and challenges of hydrogel actuators, and hopefully will motivate researchers from different fields to explore all the potentials of hydrogel actuators.

Keywords: Hydrogel; Thermo-Responsive; Actuator; Shape-Adaptive

Received 29 January 2019, **Accepted** 21 February 2019

DOI: 10.30919/es8d788

1. Introduction

Shape-adaptive hydrogel actuators, as emerging intelligent materials, possess a unique shape change property in response to different external stimuli (pH, temperature, light, force, ions, magnetic/electric field, and biochemical signals), are important for fundamental research and practical applications, including artificial muscles,¹⁻³ soft robotics,^{4,6} and human-machine interfaces.⁷⁻¹¹ As compared to other actuators made of elastomers, polymer/inorganic composites, and carbon-based materials, hydrogel actuators are particularly attractive, because hydrogels exhibit intrinsic swelling behaviors and tunable strain-induced viscoelastic, mechanical, and some self-recovery properties in highly hydrated, three dimensional porous structure,¹²⁻¹⁹ which offer them great potentials to realize a variety of reversible actuations under different stimuli.²⁰ To this end, significant and continuous efforts have been made to develop

stimuli-responsive hydrogel actuators as intelligent and programmable materials, capable of changing their shape/size/volume and probably other functional properties (e.g. conductivity, permeability, viscosity, and mechanics) in response to different stimuli.

However, challenges still remain. Since hydrogels are typically isotropic materials that usually undergo uniform volumetric expansion and contraction in response to external stimuli, they are difficult to achieve asymmetrical shape changes such as bending, twisting, and folding.²¹⁻²⁵ Use of single polymer materials or simple polymer structures are unlikely to selectively trigger site-specific swelling or contraction, leading to shape adaptability and transformation in a controllable manner. A general working principle for shape-adaptive hydrogel actuators is to create a mismatch stress within polymer network (e.g. softer vs. stiffer, swelling vs. non/less-swelling), which helps to realize the controllable shape changes for actuation. A common strategy for hydrogel actuators is to develop hybrid materials (e.g. different polymers, crosslinkers, nanofillers) into hydrogel networks, with new network structures and new actuation mechanisms. It is also equally important to develop new synthesis methods to fabricate such hydrogel actuators. In this way, upon external stimulation, different components or regions of hydrogels undergo different extents of volume expansion/contraction in certain positions or directions, thus leading to macroscopic shape changes by bending, stretching, twisting, and folding.

Different from other shapeable actuators made of alloys, elastomers, and proteins/peptides, hydrogel actuators are highly hydrophilic and contain high water content, thus shape response in hydrogels is mainly triggered in the aqueous environment of the materials, i.e. the swelling/shrinking properties of hydrogel materials need also to be compatible with external stimuli (light, temperature, pH, ions or magnetic/electric field). To this end, different types of materials including polymers, inorganic, electrical, and conductive materials can

¹ Human Key Laboratory of Biomedical Nanomaterials and Devices College of Life Sciences and Chemistry Hunan University of Technology, Zhuzhou 412007, China

² School of Materials Science and Engineering Henan Polytechnic University, Jiaozuo, 454003, China

³ College of Materials Science & Engineering Zhejiang University of Technology, Hangzhou 310014, China

⁴ School of Pharmaceutical Sciences Wenzhou Medical University, Wenzhou, Zhejiang 325035, P.R. China

⁵ Department of Chemical and Biomolecular Engineering The University of Akron, Akron, Ohio 44325

[†]The authors contribute equally to this work.

*E-mail: woody870402@hotmail.com; jxtang0733@163.com; zhengj@uakron.edu

be used, separately or in combination, to design different hydrogel-based actuators. Incorporation of two or more components in polymer networks also allows different parts of the hydrogels to be swollen and shrank at different rates in response to external signals, leading to a controllable shape change. Apart from materials itself, shape change of hydrogel actuators also depends on network structure. Different network structures including bilayer, layer-by-layer, gradient, and nanocomposite structures have been fabricated to realize programmable shape changes. Regardless of different stimuli-responsive materials and hydrogel network structures, driving forces for programmable shape change are resulted from the directional anisotropic swelling or contraction of hydrogels by changing the conformation of polymer chains to optimize the free energy of the whole system.

Research in both hydrogel and hydrogel actuator fields experiences enormous growth as evidenced by the large increase in publication over the past decade in Fig. 1. The overall growth rate in published papers was approximately 350 % for hydrogels and 630 % for hydrogel actuators in the past decade, respectively, indicating

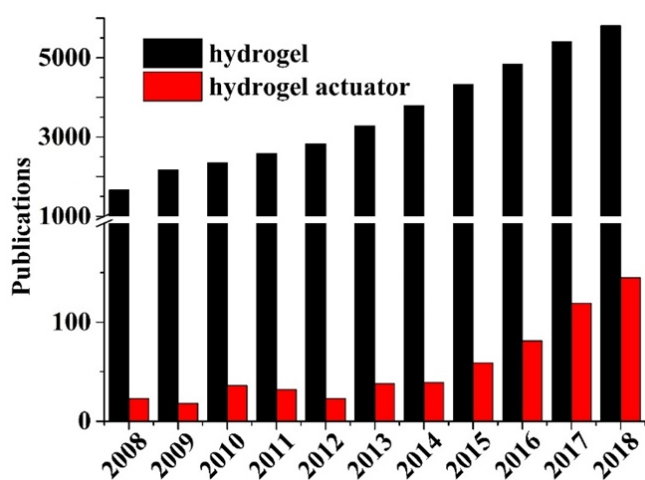


Fig. 1 Number of SCI-index papers by searching the keyword of “hydrogels” and “hydrogel actuators” from ISI database.

significant progress and high impact of the research in both fields. While the growth rate of publication in the “hydrogel actuators” subfield was almost doubled to the “hydrogel”, hydrogel actuators (not even mention to thermo-responsive hydrogel actuators) are still a subject under less investigation, and do not catch the pace of the publication in other traditional subfields on tough hydrogels, nanocomposite hydrogels, biomaterial hydrogels, etc. Thus, the continuous efforts are still needed to develop alternative hydrogel actuators.

In this review, we aim to provide an updated research summary on recent progress in the past five years and future direction in thermo-responsive, shape-adaptive hydrogel actuators, instead a comprehensive or exhaustive one. This review mainly covers fundamental principles of thermo-based shapeable actuation mechanisms, selectively highlights some intriguing and novel hydrogel actuator systems, and points out some of the persistent technological barriers and the research directions that should be undertaken to overcome these barriers. We should note that some hydrogel actuator examples could be used for different subsections due to their overlapped properties, so we prioritize them in an order of materials, structural, and responsive properties. Hopefully, this review will provide a different perspective to stimulate further research efforts for exploring all the potentials of stimuli-responsive soft materials, not limited to thermo-responsive and shape-adaptive hydrogel actuators.

2. Network Structures of Thermo-Responsive, Shape-Adaptive Hydrogel Actuators

Thermo-responsive hydrogel actuators driven by different shape-adaptive mechanisms strongly depend on their network structures. Based on a general working principle of creating the anisotropic and spatial non-uniform stresses in different regions/parts of the hydrogels, different hydrogel structures enable to realize different thermo-responsive properties and thus to achieve the fast, sensitive, and tunable actuation. To manipulate the extent of swelling/shrinkage, hydrogel structures can be mainly grouped into four categories of bilayer structure, layer-by-layer structure, gradient structure, and nanocomposite structure (Fig. 2). The former two structures are likely constructed by

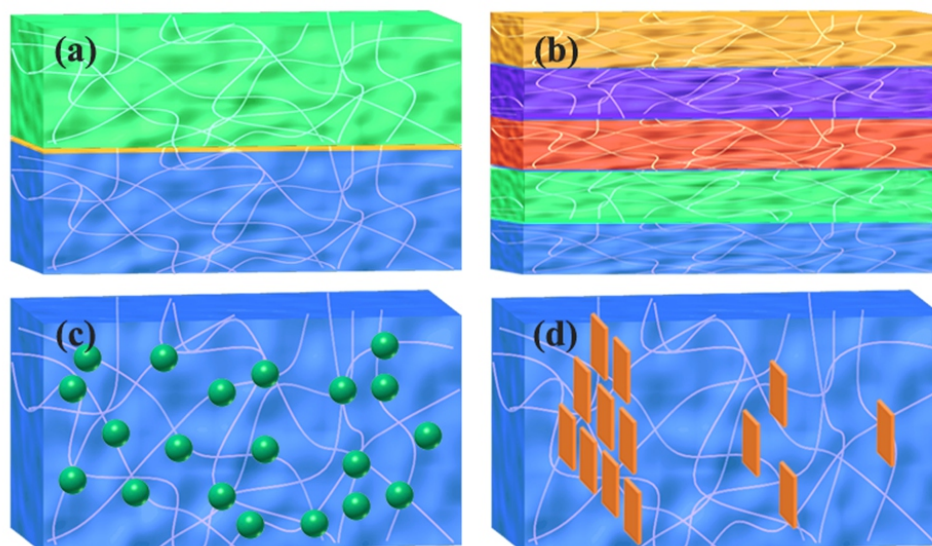


Fig. 2 Four representative network structures of shape-adaptive hydrogel actuators, including (a) bilayer, (b) layer-by-layer, (c) gradient, and (d) nanocomposite structures.

adhering two or more homogenous layers together to create an overall heterogeneous network structure. The latter two structures are often constructed by adding nanofillers or crosslinkers in a single, dominant network to create diverse crosslinked network densities along a film thickness direction. All these network structures allow to create and maximize the stress mismatch for shape actuation upon thermo-induced swelling/deswelling.

2.1. Bilayer Structure

Bilayer hydrogels, whose two layers possess different responsive properties, are considered as the most straightforward design to induce spatially non-uniform stresses for shape actuation.²⁶⁻²⁸ The presence of two heterogeneous layers, which are either physically attached or chemically crosslinked, is expected to undergo different or completely opposite swelling behaviors, which further amplify the mismatch of localized stress between the two layers and thus induce shape change in response to the demanding environmental changes. Different methods, including chemical vapor deposition (CVD),²⁹ electrophoresis,³⁰ microfluidics,³¹ and bonding of two different homogeneous hydrogel,^{32,33} have been developed for fabricating bilayer hydrogel actuators. Generally speaking, in order to maximize shape changes, the two layers are often designed in a way with different or incompatible properties, e.g. one layer could be more hydrophobic, stiffer, or less swelling, while the other is more hydrophilic, softer, or more swelling. However, it becomes a challenging to create a strong bilayer interface for bonding the two incompatible layers together.

Temperature-induced actuators (not limited to shape hydrogel actuators) are widely used smart materials. Among them, poly(*N*-isopropylacrylamide) (PNIPAM) as a classical temperature-responsive polymer has been extensively explored and introduced into hydrogel actuator systems due to its phase transition at lower critical solution temperature (LCST) around 32 °C.³⁴ PNIPAM hydrogel swells at temperatures of <LCST while shrinks at temperatures of >LCST. The sol-gel transition temperature of PNIPAM can be tweaked by altering the degree of polymerization, incorporating other composites, or copolymerizing with other polymers, all of which would change the LCST-UCST properties. Taking advantage of this unique LCST-induced sol-gel transition feature of PNIPAM, different PNIPAM-based hydrogels prepared by multi-components with gradient, bilayer or even multilayer structures were developed to realize temperature-responsive actuations, due to the mismatch of the swelling/shrinkage between the temperature-responsive layer and the non/less-responsive layer.

The first strategy to create PNIPAM-based bilayer hydrogels is to simply add different nanocomposites into PNIPAM hydrogel network, which can form a polymer-rich and nanocomposite-rich bilayer structure to achieve asynchronous thermo-induced shape change and realize some actions for capturing or moving objects. For instance, when integrating clays into PNIPAM hydrogel, PNIPAM-clay nanocomposite hydrogel was formed with a bilayer structure, and each layer contained different contents of clays (Fig. 3a). By tuning the thickness ratio of a high clay layer to a low clay layer, thermo-induced bending actuation could be achieved in a programmable manner. Since the mechanical force of PNIPAM-clay hydrogels increased with clay content, upon immersing in 40 °C water, PNIPAM-clay hydrogels favored to bend towards the thicker clay layer, leading to a significant bending degree of >180° within 2 min. Such bending was also reversible when switching water temperature from 40 °C to 25 °C.³⁵

Another strategy is to regulate the transition temperature of PNIPAM-based hydrogels by copolymerizing NIPAM with other acrylamide or acrylate-based thermosensitive polymers (e.g. *N*-[3-(dimethylamino)propyl]methacrylamide (DMAPMA) and acrylamide

(AM)). Varying DMAPMA concentrations could tune their LCST of NIPAM/DMAPMA bilayer hydrogels, e.g. with 80/20 and 95/5 molar ratios of NIPAM/DMAPMA on each layer (i.e. the N80D20 and N95D5 layers), the corresponding LCST in each layer was changed to 46.6 °C and 38.4 °C, respectively.³⁶ So, in hot water of 60 °C, the NIPAM/DMAPMA hydrogel bent toward the N95D5 side by 180° in 40 s because the deswelling of the N95D5 layer occurs much earlier than that of the N80D20 layer. However, upon switching to a water solution of 25 °C, the hydrogel uncurled to recover its original straight shape due to the higher swelling of the N95D5 layer. Similarly, copolymerization of NIPAM with AM significantly increased the LCST, leading PNIPAM/AM hydrogel to swell largely at elevated temperature. Thus, a bilayer hydrogel consisting of a pure PNIPAM layer and a hybrid PNIPAM/AM layer bent towards the pure PNIPAM layer by ~180° in 60 s at 45 °C aqueous solution.³⁷ Moreover, the LCST of PNIPAM-based hydrogels can also be tuned by ionic components. When PNIPAM network was interpenetrated by alginate network ionically cross-linked by trivalent Al³⁺ ions, the LCST of PNIPAM/alginate hydrogels could be tuned in a wide range of 22.5-32 °C in response to Al³⁺ concentration.³⁸ The resultant PNIPAM/alginate hydrogels achieved a maximum bending angle of ~140° in 50 s at relatively low temperatures of 27 °C.

Apart from bilayer hydrogel actuators where both layers contain PNIPAM, they can also be designed using two different stimuli-responsive polymers in the two layers, e.g. one layer with PNIPAM and the other without PNIPAM, or both layers do not necessarily contain PNIPAM. This design can offer dual- or multiple-responsive properties for bilayer hydrogels.³⁹⁻⁴¹ For instance, PNIPAM/PDMAEMA bilayer hydrogels possessed distinct swelling characteristics for each layer, i.e. PNIPAM layer swelled at high temperature, while PDMAEMA layer swelled at high c(H⁺) due to the protonation of amino groups. PNIPAM-PVA/PDMAEMA-PSS hydrogels possessed dual-responsive and reversible bending behaviors in response to temperatures and pH, i.e. PNIPAM-PVA/PDMAEMA-PSS hydrogels underwent 180° of bending in 60 s in 45 °C water and recovered back to its original shape in 185 s in 15 °C water, and similar pH-responsive and reversible bending was also observed when switching a solution between 0.1 M HCl and ethanol.⁴² So, PNIPAM-PVA/PDMAEMA-PSS hydrogels were further designed into a four-arm gripper to capture and release a rubber block within 1 min in response to the changes in temperature from 45 °C to 15 °C and pH from 1 to 7. Another example is to integrate thermo-responsive PNIPAM and pH-responsive poly(acrylamide)-chitosan (PAAm-CS) into bilayer hydrogels,⁴³ which responded to both temperature and pH to achieve reversible bending in between hot and cool water and between alkaline and acid conditions. A combination of a PNIPAM layer with LCST and a poly(acrylic acid-co-acrylamide) (P(AAc-co-AAm)) layer with UCST could realize even faster and more sensitive bending actuation in non-aqueous environment (Fig. 3b).⁴⁴ Due to the opposite thermal-responsiveness of the two layers, the hydrogels possessed the temperature-induced bidirectional and reversible bending between towards the PNIPAM layer by 180° in 60s at 40 °C of water and backwards the P(AAc-co-AAm) layer by 90° in 60 s at 15 °C of oil. Such enhanced bending effect was also attributed to the bidirectional water diffusion between the two layers upon heating or cooling process.

Apart from PNIPAM, poly[oligo(ethylene glycol) methyl ether methacrylate] (POEGMA) is another thermo-responsive polymer with a LCST, which is readily controlled by the ethylene glycol chain length and copolymerization degree.^{45,46} Using a scalable photopatterning to prepare POEGMA hydrogels with patterned structures allowed to realize more complex shape changes as driven by temperature-induced

swelling (Fig. 3c).⁴⁷ Beside the LCST or UCST-induced thermo-responsive polymers above, dipole–dipole and hydrogen-bonding interactions are also sensitive to temperature, thus the presence of these interactions in hydrogels can also lead to thermo-induced actuation to some extents. By integrating these thermal responsive DHIR hydrogels (acrylamide, acrylonitrile, 2-acrylamido-2-methyl-1-propanesulfonic acid, and polyethylene glycol diacrylate) with non-swelling polyurethane (PU) hydrogels into a bilayer structure, the resulting DHIR-PU hydrogels expanded their tunable temperature windows (25–60 °C) to achieve a variety of thermo-induced actuation (bending angle of -90° – 180°) by simply changing the thickness ratios of the two layers.⁴⁸ The driving force is a delicate balance between the dipole–dipole and H-bonding interactions from the DHIR layer and non-swelling strain resistance from the PU layer (Fig. 3d).

2.2. Layer-by-Layer (LbL) Structure

An extension of bilayer structure is a multiple-layer or LbL structure in hydrogels. LbL network structure in hydrogels is usually constructed via a stepwise assembly process. With the advent of the controlled radical polymerization methods, the LbL strategy can accommodate much more versatile materials and structures by the introduction of various reactive end groups into the polymers, as compared to bilayer structures. Meanwhile, the LbL strategy also brings additional challenges for precise structural control.

PNIPAM/TiNS hydrogels embedding LbL co-facially oriented electrolyte nanosheets (Ti IV) allowed to modulate anisotropic

electrostatics in response to the changes of electrostatic permittivity associated with a LCST transition (Fig. 4a). The modulated anisotropic electrostatic repulsion between the LbL nanosheets resulted in immediate extension of the gel by 170 % within a second in 50 °C water, followed by the self-recovery to its original length at 15 °C.⁴⁹ Such rapid temperature-responsive elongation and shrinkage of the hydrogel allowed to design an L-shaped symmetrical bipedal walking actuator. Additionally, the plasmonic nanostructures (i.e. gold nanoparticles (AuNP)/nanoshells (AuNS)) covered with temperature-responsive polymer brushes (e.g. PNIPAM) can be assembled into LbL structure using spin-assisted technique with poly(methacrylic acid) homopolymer (PMAA) (Fig. 4b). By changing the shape and size of gold nanostructure, plasmonic nanostructures in the hydrogel can absorb a broad light spectrum from UV/visible to near-infrared lights. Apart from thermo-responsive properties, a combination of the non-light-responsive PNIPAM/PMAA deposited between light-responsive gold plasmonic nanostructures enabled to create the anisotropic swelling/deswelling under light stimuli, i.e. it exhibited fast bending (within 2 min) toward the NP side at 532 nm wavelength and the NS side at 785 nm wavelength,⁵⁰ thus possessing both photo- and thermo-induced actuation.

2.3. Gradient Structure

Hydrogel actuators with the continuous gradient structure can also meet the requirement of thermo-responsive actuation. A general design strategy to create the gradient structures is to incorporate nanofillers or crosslinkers in a single network hydrogel and distribute them in a

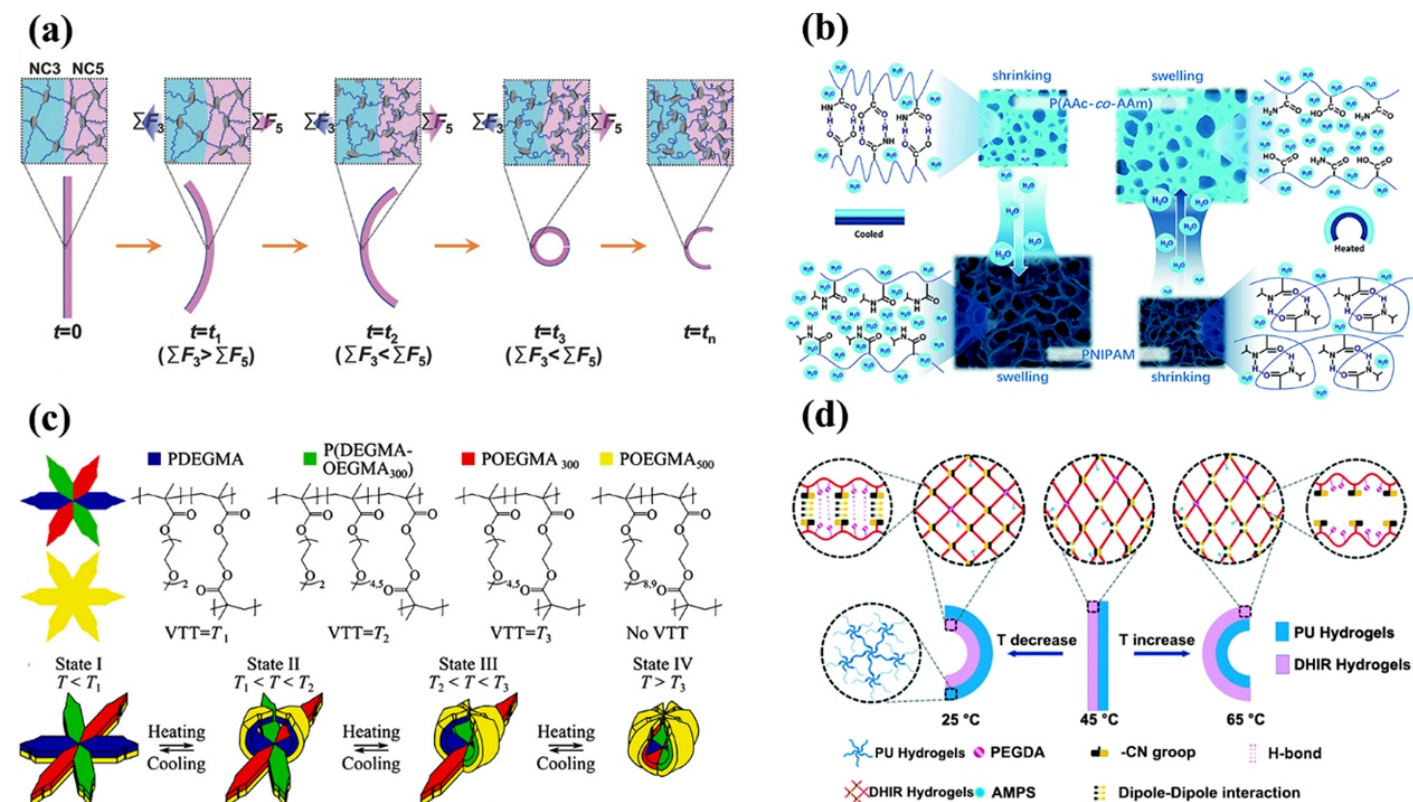


Fig. 3 Thermo-responsive bilayer hydrogel actuators. (a) Nanocomposite PNIPAM hydrogel bilayer consists of different amounts of clay in each layer (reproduced from Ref. 35, copyright 2015 WILEY-VCH); (b) PNIPAM/P(AAc-co-AAm) bilayer with opposite thermo-responsiveness offers the enhanced bidirectional bending in water and oil solutions. (reproduced from Ref.44, copyright 2018 Royal Society of Chemistry); (c) POEGMA bilayers with different chain length/copolymerization degrees exhibit different LCST to realize thermo-responsive shape change (reproduced from Ref.47, copyright 2017 WILEY-VCH); (d) DHIR-PU bilayer hydrogel consisting of a swellable DHIR layer and non-swelling PU layer is capable for thermo-induced actuation as driven by dipole–dipole and hydrogen-bonding interactions (reproduced from Ref.48, copyright 2017 Royal Society of Chemistry).

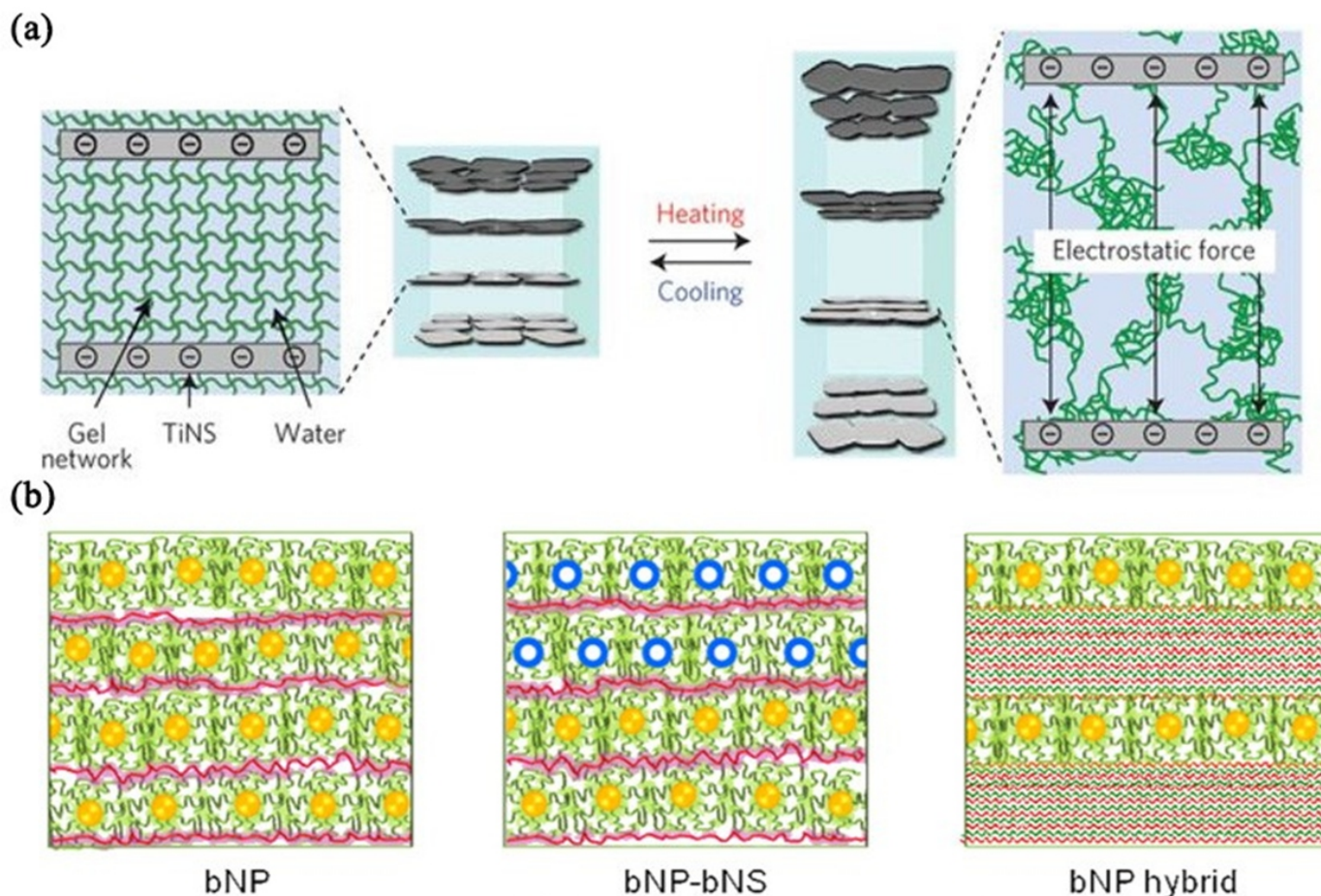


Fig. 4 Thermo-responsive hydrogel actuators with layer-by-layer structures. (a) L-shaped PNIPAM hydrogel with layer-by-layer IV nanosheet configurations exhibits a unidirectional bending (reproduced from Ref.49, copyright 2015 Springer Nature); (b) Layered PNIPAM-grafted gold-nanoparticles/nanoshells exhibit controllable photothermal actuations.(reproduced from Ref.50, copyright 2012 American Chemical Society).

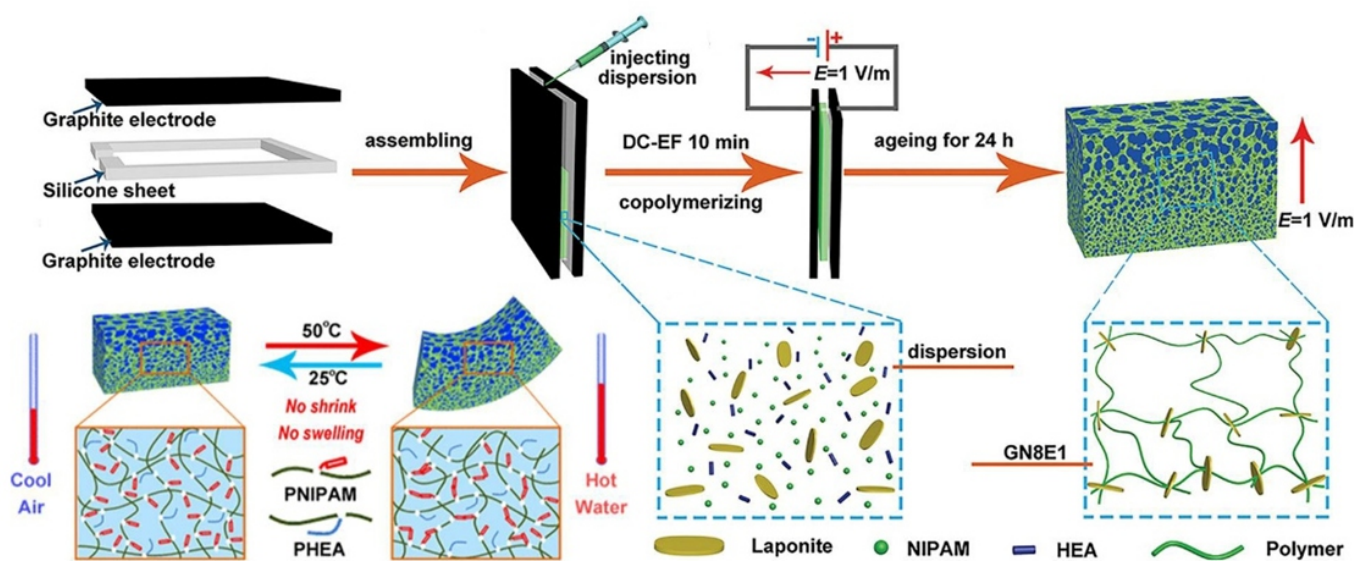


Fig. 5 Thermo-responsive hydrogel actuators with gradient structure. PNIPAM-co-HEA-Laponite hydrogel with the continuous gradient structure, prepared by external electric field, generates an asymmetric structure to realize thermo-responsive actuation (reproduced from Ref.51, copyright 2018 American Chemical Society).

gradient way to create the hydrogels with different network densities. Gradient distribution of charged laponite nanocomposites as physical crosslinkers in PNIPAM-based hydrogels allows to create an anisotropic network structure with a gradient crosslinking density. PNIPAM/Laponite gradient hydrogel actuators exhibited a rapid, large, and reversible bending of 231° in 20 s due to gradient-induced thermo-shrinkage and extension of the hydrogels (Fig. 5).⁵¹ Another gradient hydrogel actuator made of PNIPAM/hydroxyethyl acrylate (HEA) with gradient laponite also showed fast bending (40 s) in hot water (100°C) and rapid bending recovery (60 s) in air (25°C).⁵¹ Clearly, nonswelling property of laponite enables the water self-circulation (water transfer) within the hydrogel network, which help to maintain the repulsive force between the polymer chains and facilitate the swelling and bending of PNIPAM gels below the LCST. In these cases, the water self-circulation mechanism makes PNIPAM-based hydrogels to realize the actuation in water, air, or oil conditions.

2.4. Hybrid Nanocomposite Structure

The main approaches used to achieve automatic bending or folding (actuators) involve combining different materials of contrasting properties to create inhomogeneous structure. Use of nanocomposite structure by incorporating swelling polymers with non-swelling nanocomposites becomes more populated due to the ease of synthesis methods, the wide accessibility of both polymers and nanocomposites, and the contrasting nature of polymers and nanocomposites. Since nanocomposites often have a photo-thermo conversion ability, nanocomposite hydrogels usually exhibit the improved responsiveness via site-specific deformation. For example, porous doubly filled PNIPAM/SiO₂/polyaniline hydrogels displayed reversible and symmetrical shape changes in response to temperatures (swelling at 25°C and deswelling at 50°C) as fast as 6 s due to the incorporation of nano-SiO₂.⁵² By incorporating graphene oxide (GO) nanosheets, PNIPAM/GO nanocomposite hydrogels also exhibited a different actuation mechanism, in which GO nanosheets enabled to convert NIR light to heat that further induced shape actuation (Fig. 6). Upon heat transfer, PNIPAM/GO hydrogels gradually folded toward the irradiated region because the irradiated region shrunk more than the un-irradiated one. In addition, the bending degree of the hydrogels could be modulated by GO concentrations ($1.0\text{--}3.0\text{ mg}\cdot\text{mL}^{-1}$ with 90° bending in

$160\text{ s}\text{--}20\text{ s}$), hydrogel thicknesses ($1.4\text{--}2.2\text{ mm}$ with 90° bending in $27\text{ s}\text{--}99\text{ s}$), and irradiation parameters ($0.22\text{--}0.95\text{ W}\cdot\text{mm}^{-2}$ with 90° bending in $80\text{ s}\text{--}20\text{ s}$).⁵³ Following the similar line, other nanoparticles including Au and Ag NPs^{54,55} and semiconductors⁵⁶ can also be incorporated into PNIPAM hydrogels to realize the light-to-thermo-induced actuation. By introducing alginate-exfoliated WS₂ nanosheets into ice-template-polymerized PNIPAM hydrogels with cellular microstructures, WS₂ nanosheets in hydrogels exhibited strong NIR absorption to rapidly increase local temperature from room temperature to LCST within $<7\text{ s}$ under NIR radiation (808 nm , $>6\text{ W cm}^{-2}$). As a result, WS₂/PNIPAM hydrogels underwent a significant volume shrink by $\sim 90\%$ within 6 s upon exposure to NIR radiation ($\sim 6\text{ W cm}^{-2}$) at room temperature and a fully recovery within 4 s upon removal of NIR irradiation.⁵⁶

3. Multiple Temperature/Other-Stimuli Shape-Adaptive Hydrogel Actuators

Almost all of shape-adaptive hydrogels consist of multiple components, so heterogeneous materials and anisotropic structures often endow the hydrogels with multiple responsive properties and new actuation mechanisms.

3.1. Dual Thermo/Salt and Thermo/pH Responses

Some zwitterionic polymers present special intelligent responsiveness at variable salt concentrations by controlling the stretching and collapse of molecular chains. Hence, thermo/salt hydrogel actuators could be designed by the copolymerization of different unique monomers into thermo-responsive network. For instance, combination of thermo-responsive PNIPAM with salt-responsive poly(3-(1-(4-vinylbenzyl)-1H-imidazol-3-ium-3-yl)propane-1-sulfonate) (PVBIPS) allowed to fabricate PNIPAM/PVBIPS bilayer hydrogels with a pseudo-interpenetrating double-network structures at the interface using a simple one-pot method (Fig. 7a).^{31,57} Zwitterionic nature of PVBIPS also offered salt-responsive bending actuation from -370° in water to -365° in 1.0 M NaCl solution and temperature-responsive bending from 350° to 130° ($25^\circ\text{C}\text{--}55^\circ\text{C}$). Poly(2-(dimethylamino)ethyl methacrylate) (PDMAEMA-NIPAM/PDMS) bilayer hydrogels also presented a dual-responsive bidirectional bending as the changes in either temperature ($25\text{--}40^\circ\text{C}$) or pH value ($3.0\text{--}6.5$).⁴⁸ In both cases, regulating anti-polyelectrolyte effect from zwitterionic polymers, salt-responsive

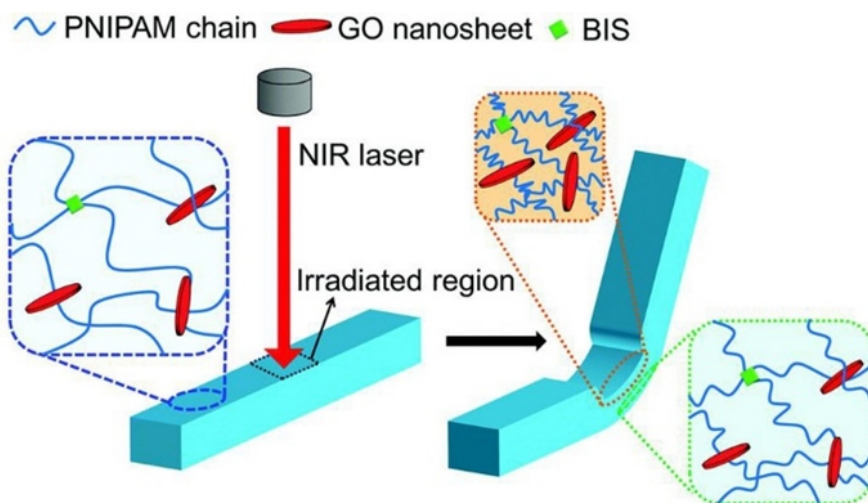


Fig. 6 Thermo-responsive nanocomposite hydrogel actuators driven by a light-to-thermo-induced actuation mechanism. PNIPAM/GO nanocomposite hydrogel exhibits the NIR-to-thermo-induced shape actuation. (reproduced from Ref.53, copyright 2017 The Royal Society of Chemistry).

actuation seems to be achieved efficiently. However, most of zwitterionic polymers are only sensitive to high salt concentrations, and the structural diversity of zwitterionic monomers is very limited. Hence, development of new thermo/salt hydrogel systems is a new research direction.

In parallel to dual thermo/salt-responsive hydrogels, thermo/pH-responsive hydrogels are also promising for practical applications. Upon

incorporating pH-responsive perylene tetracarboxylic derivative (PTCA) into an aeolotropic PNIPAM/PAAm/gelation network, the as-prepared hydrogels enabled rapid shape transformation from 220° bending at 45 °C to 70° bending at 25 °C, also accompanied by switchable “On-Off” fluorescence change (pH from 1 to 13) (Fig. 7b).⁵⁸ The introduction of polyelectrolyte components into the hydrogel structure also allows the hydrogels to achieve multiple-stimuliactuations. Triple-stimuli

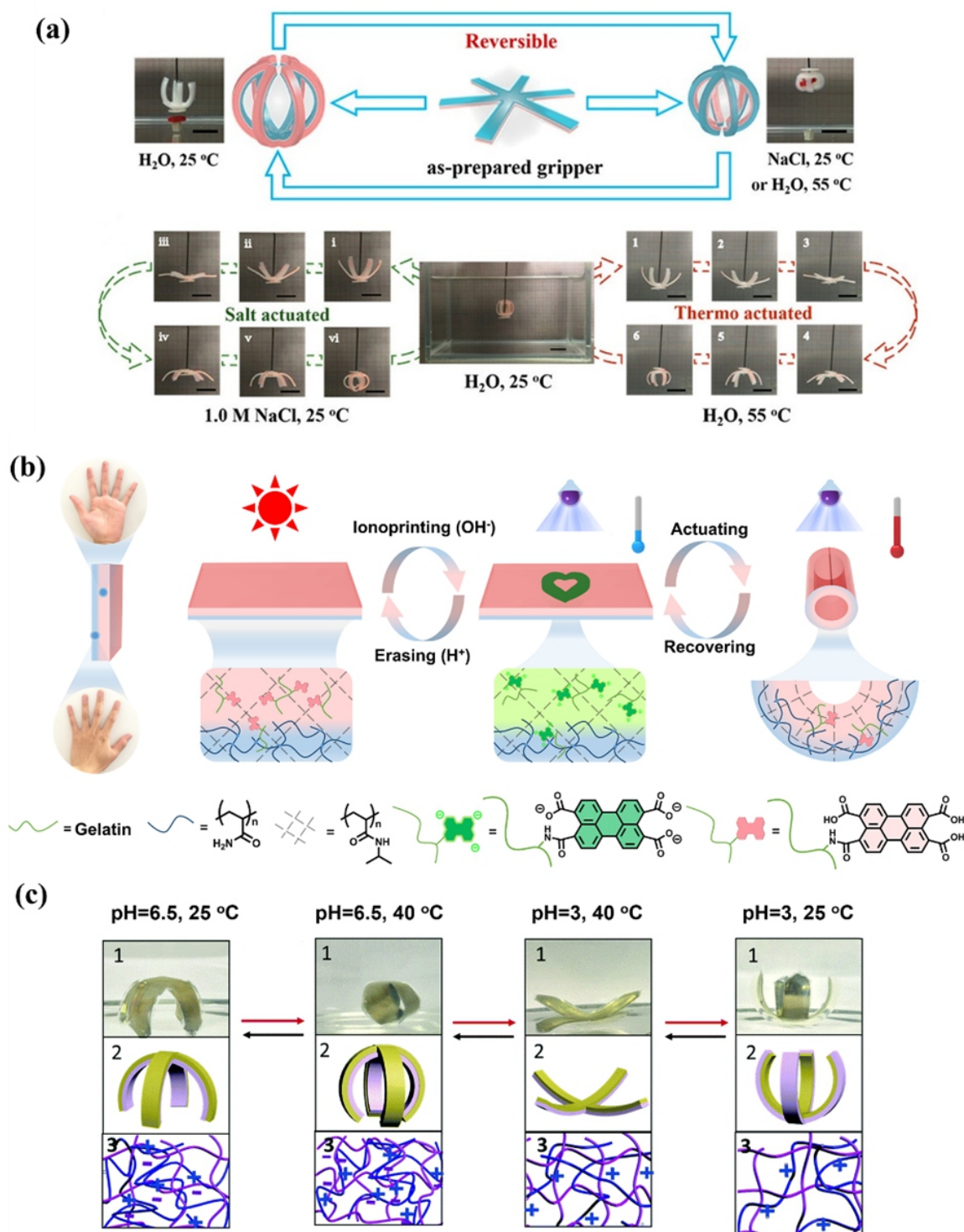


Fig. 7 Dual thermo/salt- and thermo/pH-responsive hydrogel actuators, including (a) dual thermo/salt-responsive PNIPAM/PVBIPS bilayer hydrogel (reproduced from Ref.57, copyright 2018 American Chemical Society), (b) dual thermo/pH-responsive PTCA-modified PNIPAM-PAAm hydrogel (reproduced from Ref.58, copyright 2018 WILEY-VCH), and (c) dual thermo/pH-responsive PNIPAM/PDADMAC-PDMS bilayer hydrogel (reproduced from Ref.59, copyright 2017 Royal Society of Chemistry).

anisotropic PNIPAM/PAA hydrogels exhibited repeatable, reversible, directional shape transformation in response to the changes in temperature (2–50 °C), pH (2–11), and ionic strength (0.5–2.0 M NaCl).⁵⁹ It is worth pointing out that a modified PAAm-TSMP hydrogel by incorporating azo-cyclodextrin effect and danyl-aggregation can realize shape morphing in response to the reversible variation of pH from 2.0 to 5.0 or temperature from 25 °C to 80 °C (Fig. 7c).⁶⁰ It is foreseeable that more exacting hydrogel actuators could be built by utilizing different intermolecular forces with pH-sensitivity, such as Schiff base force, conjugation, host-guest interaction, and other supramolecular interactions. Nevertheless, many thermo/pH-responsive hydrogel actuators are dedicated to macroscopic shape change, thus ignoring the change at the microscopic scale. Poly(N-isopropylacrylamide-co-maleic acid) microgels enabled reversible “inactive-active” transformation or volume shrinkage-expansion to achieve controlled drug release upon the change in either ionic triggering agents diphenhydramine (pH from 5.7 to 7.4) or temperature (4 °C to 45 °C) in PBS solution.⁶¹ Briefly, the two design strategies for thermo/pH-responsive hydrogel actuators are proposed to achieve more biomimetic applications, such as incorporating/interpenetrating pH-responsive factors into thermo-sensitive hydrogel network and selective copolymerization of monomers with both thermo/pH stimuli-responses.

3.2. Dual Thermo/Light Responses

A general design strategy to fabricate the thermo/light-responsive hydrogels is to incorporate light-absorbing nanoparticles into PNIPAM-based hydrogel network to form a hybrid nanocomposite structure, in which light-absorbing nanoparticles are capable for converting energy from light to heat so as to endow PNIPAM-based hydrogels with

light/thermo-responsive performance to induce shape changes. This design strategy has been successfully used to incorporate different light-absorbing nanoparticles (e.g. gold nanoparticles,⁶² silver nanoparticles,⁵⁴ graphene oxide,^{53,63,64} and rare-earth-oxide particles⁶⁵) into PNIPAM-based hydrogels, thus producing different dual thermo/light-responsive hydrogels. Through spatiotemporal control over the distribution of the light, these nanocomposite hydrogels were capable for achieving highly adaptable shape changes. The shape-change degree of these hydrogels can be modulated by changing the nanoparticle concentrations, hydrogel thicknesses, and irradiation power density and irradiation time. As a typical example, gold nanoparticles (AuNPs) were adsorbed into P(NIPAM-co-AAc) networks to form a light-responsive nanocomposite hydrogel (Fig. 8a). Due to surface plasmon effect of AuNPs, the resultant P(NIPAM-co-AAc) hydrogels displayed multiple shape changes in aqueous solution by controlling white-light irradiation patterns, and shape-transforming rate (τ) increased quadratically with hydrogel thickness (h_0) in terms of $\tau \sim h_0^2$. Apart from PNIPAM, a nanocomposite thermo/light-responsive hydrogel actuator was fabricated via copolymerization of stearyl acrylate (SA) and methacrylic acid (MA) with reduced graphene oxide (rGO) (Fig. 8b).⁶⁶ Upon polymerization, SA was crystallized into a dense-ordered structure, while MA was melted to induce a decrease of local network density. The local network densities were sensitive to temperatures so that the hydrogels sank in water at room temperature, but floated on water surface when temperature was increased above the melting point of MA. Furthermore, the photo-to-thermal effect via the NIR absorption by rGO would induce the melting of alkyl chains and the subsequent decrease in network density, thus leading to shape changes.

Different from nanocomposite structure, another design strategy

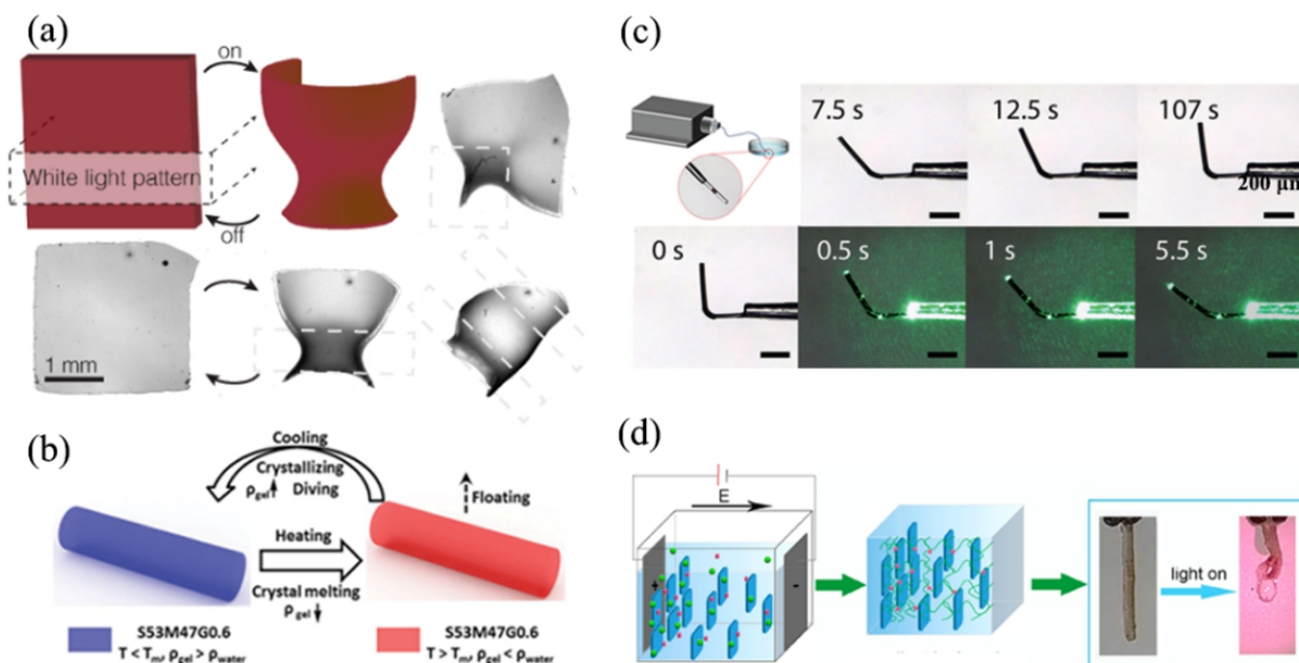


Fig. 8 Dual thermo/light-responsive hydrogel actuators, including (a) dual thermo/light-responsive AuNPs/P(NIPAM-co-AAc) nanocomposite hydrogel (reproduced with permission from Ref.62, copyright 2015 Wiley), (b) dual thermo/light-responsive rGO/P(SA-co-MA) nanocomposite hydrogel (reproduced from Ref.66, Copyright 2015 John Wiley & Sons, Inc.), (c) dual thermo/light-responsive AuNPs-PNIPAM/PAAc bilayer hydrogel (reproduced with permission from Ref.72, copyright 2016 Wiley), and (d) dual thermo/light-responsive GO/PNIPAM gradient hydrogel (reproduced with permission from Ref.73, Copyright 2018, American Chemical Society)

is to create a bilayer structure, where one layer is formed by thermo-responsive PNIPAM materials with light-absorbing nanoparticles, while the other is non-responsive layer. Using this strategy, various PNIPAM-based bilayer hydrogels have been realized by combining PNIPAM-based hydrogel matrices with different light-absorbing nanoparticles (e.g. AuNPs,⁶⁷ GO,⁶⁸ rGO,⁶⁹ and magnetite nanoparticles).^{70, 71} Most of these bilayer hydrogels can achieve asynchronous thermo/light-induced shape changes, some of which can enable to capture or move objects. For instance, a micropatterned PNIPAM-based bilayer hydrogel consisting of a PNIPAM/AuNPs composite layer and a PAA csacrificial layer was fabricated into a planar micro-actuator, which exhibited a fast light-induced bending of 60° within 1 s because PNIPAM and PAA layers exhibited different swelling properties in response to temperature and light irradiation in aqueous environments. (Fig. 8c).⁷² In addition to bilayer and

nanocomposite structures, it was reported to create a gradient concentration of GO inside PNIPAM hydrogels using an external electric field (Fig. 8d).⁷³ The resultant PNIPAM/GO hydrogels reached a maximum bending degree of 274° under NIR radiation (2 W·cm⁻²) due to the oriented GO distribution structure. Despite a great advance, it is still challenging for hydrogel actuators to complete some complicated, reversible, and robust movements, not only limited to bending behaviors.

4. Conclusions and Perspectives

Throughout a decade research, shapeable hydrogel actuators have attracted the growing interest as excellent intelligent materials for their promising applications in sensor, smart valve, circuit controller, and programmable gripper. Significant advance has been achieved in the

Table 1 Thermo-responsive hydrogel actuators with various network structure and properties.

System	Stimuli	Bending angle	Structure	Other properties
PNIPAM-clay ³⁵	40 °C	180° / 120s	Bilayer: PNIPAM with different clay concentration	N/A
PNIPAM-PDMPMA ³⁶	60 °C	180° / 40s	Bilayer with different NIPAM and DMAPMA concentration	Controllable jump
PNIPAM/PNIPAM -AM ³⁷	45 °C	180° / 60s	Bilayer	Salt responsive
alginate -PNIPAM/Al -alginate-PNIPAM ³⁸	>27 °C	140° / 50s	Bilayer	Tunable LCST with different AlCl ₃ concentration
PNIPAM/PDMPMA ⁴²	45 °C	180° / 60s	Bilayer	pH responsive
PNIPAM/ PAAm -chitosan ⁴³	45 °C	180° / 300s	Bilayer	pH responsive; shape memory
PNIPAM/P(AAc-co-AAm) ⁴⁴	40 °C	180° / 60s	Bilayer	Able to operate out of aqueous environment
PNIPAM/PVBIPS ⁵⁷	55 °C 25 °C	400° / N/A -400° / N/A	One-pot bilayer	Bidirection; Salt responsive
PDEGMA ⁴⁷	Multi -transition temperature: 18 °C, 35 °C, 50 °C	N/A (Multi-stage self-folding)	Layers of POEGMA gels with varied side chain length and extent of copolymerization	multistate shape change at different temperature
PU/PAAm-AN-AMPS ⁴⁸	60 °C 25 °C	90° / N/A -90° / N/A	Bilayer: dipole-dipole and H-bonding interaction reinforced AAm-AN-AMPS layer with non-swelling polyurethane	Bidirection; Mechanically tough
PNIPAM-co-HEA-Laponite ⁵¹	50 °C	100° / 40s	Gradient structure formed under current electric field	no shrink above LCST, with rapid recovery in air

design and synthesis of new actuatable materials with new network structures and new actuation mechanisms. Compared to other shape memory materials (e.g. alloys, elastomers, proteins/peptides, and nanocomposite), hydrogel actuators added advantages such as high stretchability, shock adsorbing, low sliding friction, and swelling/deswelling, all of which contribute to the convenient and programmable shape changes. Despite great success to date, the research in shapeable hydrogel actuators is still at its early stage as compared to other hydrogel-based materials. Some challenges still remain to be tackled before the widespread applications of shapeable hydrogel actuators become possible. As always, it is fundamentally important for the precise synthesis of programmable stimuli-responsive materials and the tracking of their stimuli and response in the complex milieu. Apart from this obvious point, we offer some personal perspectives regarding challenges and future research for shapeable hydrogel actuators.

First, high water content in hydrogels makes them mechanically weak and brittle. This weakness greatly limits the extent, time, and reversibility of shape actuation because the hydrogels require a minimal mechanical strength to withstand actuation-induced deformation. Further efforts are needed to improve the mechanical properties of hydrogels. While different tough hydrogels, such as double network hydrogels,⁷⁵ nanocomposite hydrogels,⁷⁶⁻⁷⁸ microparticle-incorporated hydrogels,⁷⁹ hydrophobically associated hydrogels,^{80, 81} and ionically cross-linked hydrogels,⁸² mechanically toughness and shapeable actuation appear to be the two highly desirable, but different properties of polymer hydrogels. Most of hydrogels still possess either property, i.e. most of actuatable hydrogels are not tough hydrogels, and *vice versa*. Thus, development of stimuli-responsive and mechanical strong hydrogel actuators is critical for many applications, but still in its infant stage. Here we suggest two possible working strategies to achieve mechanically strong and shape-adaptive hydrogels by (i) incorporate in stimuli-responsive polymers with other mechanically-enhanced nanofillers or composites and (ii) creating new network structures with better energy dissipation and reversible network recovery.

Second, most of hydrogel actuators are hybrid systems with anisotropic structures in order to achieve shape changes. However, achieving the fast and reversible shape actuation still remains to be a big challenge. Simple mixing, copolymerization, or crosslinking of different components in hybrid hydrogels often fail to construct a programmable or reversible shape change in response to external stimuli. Thus, introduction of non-covalent crosslinkers and interactions (e.g. hydrogen bonding, ionic/electrostatic interactions, hydrophobic interactions, self-assembly) may offer the more proper molecular and structural designs for reversible/programmable shape changes. Also, physical interactions could allow hydrogel actuators to recover to their original shape, structure, and functionality in multiple times without largely compromising their mechanical properties or other properties (e.g. self-healing, biocompatibility). In the case of hydrogel actuators with a bilayer structure, the bonding process to join the two hydrogels together and to form a strong bilayer interface is challenging. A possible strategy is to borrow a double-network concept to create a bilayer interface composed of different polymer chains interpenetrating with each other, which help to realize the strong bonding of the two layers of the hydrogels.

Third, NIPAM-based hydrogels are the most commonly used to fabricate hydrogel actuators, due to their favorable phase transition at LCST, facile preparation, and high biocompatibility. NIPAM-based hydrogel actuators often suffer from their low mechanical strength, slow response and recovery, narrow LCST of around 32 °C, which greatly limit their practical applications. Certainly, seeking other thermal-responsive materials also plays an important role in the

development of practical hydrogel actuators.

Fourth, another big challenge, which was not discussed in-depth in this review but has great potential, is to link hydrogel actuators with applications. When applying hydrogel actuators to specific applications, additional concerns need to be considered and addressed. For instance, use of programmable hydrogel actuators for human-machine interfaces needs to overcome some limits and/or add some new functions, e.g. increase of surface adhesion for skin sensors, integration and miniaturization of electronic circuit into hydrogel actuators for electronic devices, the biocompatibility and biodegradability of hydrogel actuators for implants, tissue scaffolds, and drug/gene delivery carriers, and 3D/4D printing of these smart hydrogel actuators into different objects. In addition, the use of computational and machine learning technologies can potentially impact the structure-based design of hydrogel actuators with the improved prediction for their optimal properties, desirable functions, and accurate/controllable shape actuations in complex environment.

Acknowledgement

J. Z. thanks financial supports from NSF (DMR-1806138 and CMMI-1825122).

Reference

1. K. P. Liles, A. F. Greene, M. K. Danielson, N. D. Colley, A. Wellen, J. M. Fisher and J. C. Barnes, *Macromol. Rapid Commun.*, 2018, 1700781.
2. C. Yang and Z. Suo, *Nat. Rev. Mater.*, 2018, 3, 125-142.
3. Z. Zhao, R. Fang, Q. Rong and M. Liu, *Adv. Mater.*, 2017, 29, 1703045.
4. Y. Zhou, C. Wan, Y. Yang, H. Yang, S. Wang, Z. Dai, K. Ji, H. Jiang, X. Chen and Y. Long, *Adv. Func. Mater.*, 2018, 1806220.
5. H. I. s. Thérien-Aubin, Z. L. Wu, Z. Nie and E. Kumacheva, *J. Am. Chem. Soc.*, 2013, 135, 4834-4839.
6. C. Yang, W. Wang, C. Yao, R. Xie, X. J. Ju, Z. Liu and L. Y. Chu, *Sci. Rep.*, 2015, 5, 13622.
7. Z. Lei, Q. Wang, S. Sun, W. Zhu and P. Wu, *Adv. Mater.*, 2017, 29, 1700321.
8. H. Ko and A. Javey, *Accounts Chem. Res.*, 2017, 50, 691-702.
9. M. Liao, P. Wan, J. Wen, M. Gong, X. Wu, Y. Wang, R. Shi and L. Zhang, *Adv. Func. Mater.*, 2017, 27, 1703852.
10. D. L. Taylor and M. In Het Panhuis, *Adv. Mater.*, 2016, 28, 9060-9093.
11. X. Le, W. Lu, J. Zhang and T. Chen, *Adv. Sci.*, 2019, 7, 1801584.
12. P. Li, D. Zhang, Y. Zhang, W. Lu, W. Wang and T. Chen, *ACS Sens.*, 2018, 3, 2394-2401.
13. D. Zhang, Y. Fu, L. Huang, Y. Zhang, B. Ren, M. Zhong, J. Yang and J. Zheng, *J. Mater. Chem. B*, 2018, 6, 950-960.
14. W. Lu, C. Ma, D. Zhang, X. Le, J. Zhang, Y. Huang, C. F. Huang and T. Chen, *J. Phys. Chem. C*, 2018, 122, 9499-9506.
15. M. D. Konieczynska, J. C. Villacampo, C. Ghobril, M. Perezviloria, K. M. Tevis, W. A. Blessing, A. Nazarian, E. K. Rodriguez and M. W. Grinstaff, *Angew. Chem. Int. Ed.*, 2016, 55, 9984-9987.
16. N. Roy, N. Saha, T. Kitano and P. Saha, *Soft. Matter.*, 2010, 8, 130-148.
17. B. Mirani, E. Pagan, B. Currie, M. A. Siddiqui, R. Hosseinzadeh, P. Mostafalu, Y. S. Zhang, A. Ghahary and M. Akbari, *Adv. Healthc. Mater.*, 2017, 6, 1700718.
18. S. Sakai, M. Tsumura, M. Inoue, Y. Koga, K. Fukano and M. Taya, *J. Mater. Chem. B*, 2013, 1, 5067-5075.
19. D. Zhang, Y. Zhang, W. Lu, X. Le, P. Li, L. Huang, J. Zhang, J. Yang, M. J. Serpe, D. Chen and T. Chen, *Adv. Mater. Technol.*, 2019, 4, 1800201.
20. T. S. Stashak, E. Farstvedt and A. Othic, *Clin. Tech. Equine Pract.*, 2004, 3, 148-163.
21. C. J. Lee, H. Wu, Y. Hu, M. Young, H. Wang, D. Lynch, F. Xu, H. Cong and G. Cheng, *ACS Appl. Mater. Interfaces*, 2018, 10, 5845-5852.
22. H. Wang, Y. Hu, D. Lynch, M. Young, S. Li, H. Cong, F. J. Xu and G. Cheng, *ACS Appl. Mater. Interfaces*, 2018, 10, 37609-37617.
23. B. Cao, C. J. Lee, Z. Zeng, F. Cheng, F. Xu, H. Cong and G. Cheng, *Chem. Sci.*, 2016, 7, 1976-1981.

24. B. Cao, Q. Tang, L. Li, C. J. Lee, H. Wang, Y. Zhang, H. Castaneda and G. Cheng, *Chem. Sci.*, 2015, **6**, 782-788.
25. C. J. Lee, H. Wang, M. Young, S. Li, F. Cheng, H. Cong and G. Cheng, *Acta Biomater.*, 2018, **75**, 161-170.
26. G. Stoychev, N. Pureskiy and L. Ionov, *Soft Matter*, 2011, **7**, 3277-3279.
27. V. Stroganov, S. Zakharchenko, E. Sperling, A. K. Meyer, O. G. Schmidt and L. Ionov, *Adv. Func. Mater.*, 2014, **24**, 4357-4363.
28. J. Zhang, J. Wu, J. Sun and Q. Zhou, *Soft Matter*, 2012, **8**, 5750-5752.
29. M. S. Oh, Y. S. Song, C. Kim, J. Kim, J. B. You, T. S. Kim, C. S. Lee and S. G. Im, *ACS Appl. Mater. Interfaces*, 2016, **8**, 8782-8788.
30. Z. Li, Y. Su, B. Xie, H. Wang, T. Wen, C. He, H. Shen, D. Wu and D. Wang, *J. Mater. Chem. B*, 2013, **1**, 1755-1764.
31. K. D. Seo, J. Doh and D. S. Kim, *Langmuir*, 2013, **29**, 15137-15141.
32. L. Zhao, J. Huang, Y. Zhang, T. Wang, W. Sun and Z. Tong, *ACS Appl. Mater. Interfaces*, 2017, **9**, 11866-11873.
33. W. J. Zheng, N. An, J. H. Yang, J. Zhou and Y. M. Chen, *ACS Appl. Mater. Interfaces*, 2015, **7**, 1758-1764.
34. E. S. Gil and S. M. Hudson, *Prog. Polym. Sci.*, 2004, **29**, 1173-1222.
35. C. Yao, Z. Liu, C. Yang, W. Wang, X. J. Ju, R. Xie and L.-Y. Chu, *Adv. Func. Mater.*, 2015, **25**, 2980-2991.
36. G. Gao, Z. Wang, D. Xu, L. Wang, T. Xu, H. Zhang, J. Chen and J. Fu, *ACS Appl. Mater. Interfaces*, 2018, **10**, 41724-41731.
37. Y. Cheng, C. Huang, D. Yang, K. Ren and J. Wei, *J. Mater. Chem. B*, 2018, **6**, 8170-8179.
38. W. J. Zheng, N. An, J. H. Yang, J. Zhou and Y. M. Chen, *ACS Appl. Mater. Interfaces*, 2015, **7**, 1758-1764.
39. J. H. Na, N. P. Bende, J. Bae, C. D. Santangelo and R. C. Hayward, *Soft Matter*, 2016, **12**, 4985-4990.
40. L. Zhang, P. E. Naumov, X. Du, Z. Hu and J. Wang, *Adv. Mater.* 2017, **29**, 1702231.
41. D. Kim, H. S. Lee and J. Yoon, *Sci. Rep.*, 2016, **6**, 20921.
42. Y. Cheng, K. Ren, D. Yang and J. Wei, *Sensors Actuat. B-Chem.*, 2018, **255**, 3117-3126.
43. L. Wang, Y. Jian, X. Le, W. Lu, C. Ma, J. Zhang, Y. Huang, C.-F. Huang and T. Chen, *Chem. Commun.*, 2018, **54**, 1229-1232.
44. J. Zheng, P. Xiao, X. Le, W. Lu, P. Théato, C. Ma, B. Du, J. Zhang, Y. Huang and T. Chen, *J. Mater. Chem. C*, 2018, **6**, 1320-1327.
45. S. Han, M. Hagiwara and T. Ishizone, *Macromolecules*, 2003, **36**, 8312-8319.
46. J. F. Lutz, Ö. Akdemir and A. Hoth, *J. Am. Chem. Soc.*, 2006, **128**, 13046-13047.
47. K. Kobayashi, S. H. Oh, C. Yoon and D. H. Gracias, *Macromol. Rapid Commun.*, 2018, **39**, 1700692.
48. H. Jia, Z. Huang, Z. Fei, P. J. Dyson, Z. Zheng and X. Wang, *J. Mater. Chem. B*, 2017, **5**, 8193-8199.
49. Y. S. Kim, M. Liu, Y. Ishida, Y. Ebina, M. Osada, T. Sasaki, T. Hikima, M. Takata and T. Aida, *Nat. Mater.*, 2015, **14**, 1002.
50. Z. Zhu, E. Senses, P. Akcora and S. A. Sukhishvili, *ACS Nano*, 2012, **6**, 3152-3162.
51. Y. Tan, D. Wang, H. Xu, Y. Yang, X.-L. Wang, F. Tian, P. Xu, W. An, X. Zhao and S. Xu, *ACS Appl. Mater. Interfaces*, 2018, **10**, 40125-40131.
52. K. Depa, A. Strachota, M. Šlouf, J. Brus and V. Cimrová, *Sensors Actuat. B-Chem.*, 2017, **244**, 616-634.
53. X. Peng, T. Liu, C. Jiao, Y. Wu, N. Chen and H. Wang, *J. Mater. Chem. B*, 2017, **5**, 7997-8003.
54. H. Guo, J. Cheng, J. Wang, P. Huang, Y. Liu, Z. Jia, X. Chen, K. Sui, T. Li and Z. Nie, *J. Mater. Chem. B*, 2017, **5**, 2883-2887.
55. X. Du, H. Cui, B. Sun, J. Wang, Q. Zhao, K. Xia, T. Wu and M. S. Humayun, *Adv. Mater. Technol.*, 2017, **2**, 1700120.
56. L. Zong, X. Li, X. Han, L. Lv, M. Li, J. You, X. Wu and C. Li, *ACS Appl. Mater. Interfaces*, 2017, **9**, 32280-32289.
57. S. Xiao, M. Zhang, X. He, L. Huang, Y. Zhang, B. Ren, M. Zhong, Y. Chang, J. Yang and J. Zheng, *ACS Appl. Mater. Interfaces*, 2018, **10**, 21642-21653.
58. B. Y. Wu, X. X. Le, Y. K. Jian, W. Lu, Z. Y. Yang, Z. K. Zheng, P. Theato, J. W. Zhang, A. Zhang and T. Chen, *Macromol. Rapid Commun.*, 2018, **13**, 1800648.
59. J. Shang and P. Theato, *Soft Matter*, 2018, **14**, 8401-8407.
60. Y. Y. Xiao, X. L. Gong, Y. Kang, Z. C. Jiang, S. Zhang and B. J. Li, *Chem. Commun.*, 2016, **52**, 10609-10612.
61. G. Fundueanu, M. Constantin, S. Bucataru and P. Ascenzi, *Polymer*, 2017, **110**, 177-186.
62. A. W. Hauser, A. A. Evans, J. H. Na and R. C. Hayward, *Angew. Chem. Int. Ed. Engl.*, 2015, **54**, 5434-5437.
63. K. Shi, Z. Liu, Y. Y. Wei, W. Wang, X. J. Ju, R. Xie and L. Y. Chu, *ACS Appl. Mater. Interfaces*, 2015, **7**, 27289-27298.
64. C. Ma, X. Le, X. Tang, J. He, P. Xiao, J. Zheng, H. Xiao, W. Lu, J. Zhang, Y. Huang and T. Chen, *Adv. Func. Mater.*, 2016, **26**, 8670-8676.
65. S. Watanabe, H. Era and M. Kunitake, *Sci. Rep.*, 2018, **8**, 13528.
66. L. Wang, Y. Liu, Y. Cheng, X. Cui, H. Lian, Y. Liang, F. Chen, H. Wang, W. Guo, H. Li, M. Zhu and H. Ihara, *Adv. Sci.*, 2015, **2**, 1500084.
67. Q. Shi, H. Xia, P. Li, Y. S. Wang, L. Wang, S. X. Li, G. Wang, C. Lv, L. G. Niu and H. B. Sun, *Adv. Opt. Mater.*, 2017, **5**, 1700442.
68. E. Zhang, T. Wang, W. Hong, W. Sun, X. Liu and Z. Tong, *J. Mater. Chem. A*, 2014, **2**, 15633.
69. D. Kim, H. S. Lee and J. Yoon, *Sci. Rep.*, 2016, **6**, 20921.
70. E. Lee, D. Kim, H. Kim and J. Yoon, *Sci. Rep.*, 2015, **5**, 15124.
71. D. Kim, H. Kim, E. Lee, K. S. Jin and J. Yoon, *Chem. Mater.*, 2016, **28**, 8807-8814.
72. Y. Zhou, A. W. Hauser, N. P. Bende, M. G. Kuzyk and R. C. Hayward, *Adv. Func. Mater.*, 2016, **26**, 5447-5452.
73. Y. Yang, Y. Tan, X. Wang, W. An, S. Xu, W. Liao and Y. Wang, *ACS Appl. Mater. Interfaces*, 2018, **10**, 7688-7692.
74. A. W. Hauser, A. A. Evans, J. H. Na and R. C. Hayward, *Angew. Chem. Int. Ed.*, 2015, **54**, 5434-5437.
75. J. P. Gong, Y. Katsuyama, T. Kurokawa and Y. Osada, *Adv. Mater.*, 2003, **15**, 1155-1158.
76. K. Haraguchi and T. Takehisa, *Adv. Mater.* 2002, **14**, 1120-1124.
77. K. Xu, J. Wang, Q. Chen, Y. Yue, W. Zhang and P. Wang, *J. Colloid Interf. Sci.*, 2008, **321**, 272-278.
78. G. Gao, G. Du, Y. Sun and J. Fu, *ACS Appl. Mater. Interfaces*, 2015, **7**, 5029-5037.
79. T. Huang, H. G. Xu, K. X. Jiao, L. P. Zhu, H. R. Brown and H. L. Wang, *Adv. Mater.*, 2007, **19**, 1622-1626.
80. W. Li, H. An, Y. Tan, C. Lu, C. Liu, P. Li, K. Xu and P. Wang, *Soft Matter*, 2012, **8**, 5078-5086.
81. S. Abdurrahmanoglu, V. Can and O. Okay, *Polymer*, 2009, **50**, 5449-5455.
82. T. L. Sun, T. Kurokawa, S. Kuroda, A. B. Ihsan, T. Akasaki, K. Sato, M. A. Haque, T. Nakajima and J. P. Gong, *Nat. Mater.*, 2013, **12**, 932-937.

Publisher's Note Engineered Science Publisher remains neutral with regard to jurisdictional claims in published maps and institutional affiliations.